Theoretical Study on H_2-Induced Acetaldehyde Elimination from $CH_3(O)CCo(CO)_3$

Louis Versluis and Tom Ziegler*

Department of Chemistry, University of Calgary, Calgary, Alberta, Canada T2N 1N4

Received April 2, 1990

Approximate Density Functional calculations have been carried out on the addition of H_2 to $CH_3(O)CCo(CO)_3$ as well as the product elimination step in which $CH_3(O)CH$ and $HCo(CO)_3$ are subsequently formed. These reactions represent the last step, e, of the catalytic hydroformylation cycle according to the mechanism proposed by Heck and Breslow. H_2 was found to form stable bipyramidal η^2 adducts with the coordinatively unsaturated acyl intermediate $CH_3(O)CCo(CO)_3$. The η^2 adducts have in the optimized structures of lowest energy the acyl group positioned along the apical axis and the H_2 molecule coordinated in the equatorial site. The adduct with H_2 lying in the basal plane was found to be only 19 kJ/mol lower in energy than the corresponding complex with H_2 parallel to the apical axis. The dihydride complex that results from an oxidative addition of H_2 by way of the most stable η^2-H_2 structure was calculated to be less stable than the parent η^2 adduct by 25 kJ/mol. The higher stability of the η^2-H_2 complex in comparison to the dihydride was attributed to the stabilization of the cobalt d orbitals by the π-accepting CO ligands. The oxidative addition reaction was investigated further by modeling the energy profile with a linear transit procedure. The profile from the linear transit revealed an activation energy ΔE^* of 77 kJ/mol. The activation energy stems primarily from the stretching of the H–H bond during the initial stages of the reaction. The total activation energy for step e along the oxidative addition/reductive elimination path was calculated to be 77 kJ/mol, with the oxidative addition being rate determining. Step e was also studied for an alternative mechanism in which the η^2-H_2 complex is converted to an aldehyde molecule and the catalyst $HCo(CO)_3$ by direct hydrogen transfer from the coordinated H_2 molecule to the acyl ligand. A stable intermediate in which H_2 has moved toward the acyl group, thereby forming a four-center species, was found to be 83 kJ/mol higher in energy than the initial η^2-H_2 compound. The corresponding reaction profile, modeled by a linear transit procedure, revealed only a minimal activation barrier. The subsequent separation of the molecular structure into the products resulted in a decrease of the energy. Both mechanisms for step e seem to be viable. On the basis of these results, the activation energy for the entire process, $H_2 + CH_3(O)CCo(CO)_3 \rightarrow CH_3(O)CH + HCo(CO)_3$, was estimated to be ~75–85 kJ/mol. This value is of the same order of magnitude as the activation energy for the oxidative addition reaction. Furthermore, it is also comparable to the activation energy of the preceding catalytic reaction step in the hydroformylation cycle, alkyl migration.

I. Introduction

The oxo or hydroformylation reaction has been utilized for more than 50 years to convert olefins and synthesis gas into aldehydes on a large industrial scale.[1] The process, which was discovered in 1938 by Roelen, is catalyzed homogeneously by low-valent cobalt[1] or rhodium[2] complexes. The most commonly used (pre)catalyst is $HCo(CO)_4$, which is generated in situ from the hydrogenation of $Co_2(CO)_8$ by H_2.

The most widely accepted mechanism for the cobalt-based hydroformylation process is due to Heck and Breslow;[3] see Scheme I. The catalytic cycle in Scheme I consists of a number of elementary reaction steps (a–e) of which a–d have been investigated in two previous theoretical studies[4] from this laboratory.

The last step in the catalytic cycle of the hydroformylation process, e of Scheme I, is the reaction of the acyl intermediate with H_2, which results in the formation of the desired aldehyde molecule and regeneration of the catalyst $HCo(CO)_3$.

There are several possible routes by which the aldehyde product can be formed from the acyl intermediate. Heck

Scheme I

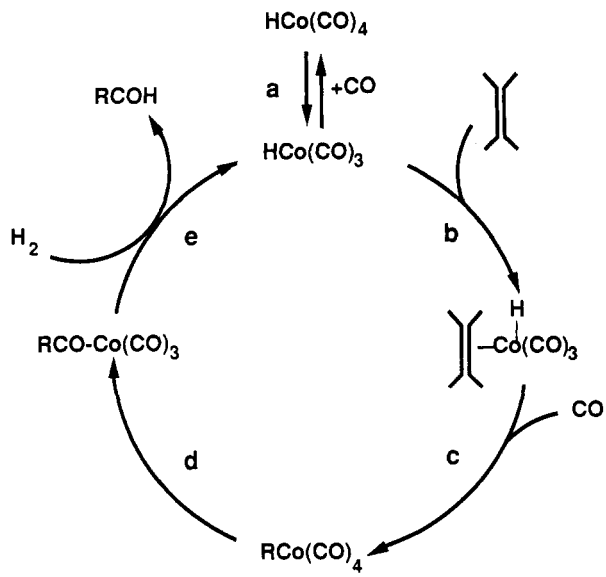

and Breslow[3] proposed a mechanism in which the coordinatively unsaturated acyl complex first undergoes an oxidative addition of H_2, affording a dihydro acyl compound (eq 1), followed by irreversible reductive elimination of an aldehyde molecule (eq 2).

$$R(O)CCo(CO)_3 + H_2 \rightarrow R(O)CCo(CO)_3(H)_2 \quad (1)$$

$$R(O)CCo(CO)_3(H)_2 \rightarrow RCHO + HCo(CO)_3 \quad (2)$$

This type of process has been inferred for numerous catalytic and stoichiometric systems.[5] It is thus not

(1) (a) Heck, R. F. *Adv. Organomet. Chem.* **1966**, *4*, 243. (b) Orchin, M.; Rupilius, W. *Catal. Rev.* **1972**, *6*, 85. (c) Orchin, M. *Acc. Chem. Res.* **1981**, *14*, 25.

(2) Pino, P.; Piacenti, F.; Bianchi, M. In *Organic Synthesis via Metal Carbonyls*; Wender, I., Pino, P., Eds.; Wiley: New York, 1977; Vol. II, pp 43–135.

(3) Heck, R. F.; Breslow, D. S. *J. Am. Chem. Soc.* **1961**, *83*, 4023.

(4) (a) Versluis, L.; Ziegler, T.; Baerends, E. J.; Ravenek, W. *J. Am. Chem. Soc.* **1989**, *111*, 2018. (b) Versluis, L.; Ziegler, T.; Fan, L., submitted for publication. (c) Versluis, L. Ph.D. Thesis, University of Calgary, Canada, 1989.

0276-7333/90/2309-2985$02.50/0

surprising that they have been studied extensively by experimental[6-8] as well as theoretical[9-11] techniques. However, it has not been established that the formation of the product RCHO in fact proceeds via the oxidative addition/reductive elimination mechanism in the case of the cobalt-based hydroformylation process. The reductive elimination process of eq 2 will be investigated in section VI.

Some experimental observations indicate[12,13] that the acyl complex might react with $HCo(CO)_4$, thereby forming an aldehyde molecule and a binuclear cobalt compound (eq 3). In a subsequent reaction, $Co_2(CO)_8$ is then according to eq 4 transformed back to the mononuclear

$$R(O)CCo(CO)_3 + HCo(CO)_4 \xrightarrow{CO} RCHO + Co_2(CO)_8 \quad (3)$$

$$Co_2(CO)_8 + H_2 \rightarrow 2HCo(CO)_4 \quad (4)$$

hydrido-cobalt complex. Experimental studies of the stoichiometric reactions,[14] eqs 3 and 4, revealed that the process is very facile. However, under catalytic conditions, one has to take into account that the overall concentration of cobalt species is low in comparison to the reactants. That is, the probability for the reaction between two cobalt complexes is small.

For electron-poor systems such as early-transition-metal complexes,[15] the hydrogenolysis of the M–C bond proceeds via a mechanism in which an incoming H_2 molecule initially forms a η^2-adduct with the metal complex, followed by the concerted cleavage of the hydrogen bond and the formation of H–M and H–C bonds by way of a four-center intermediary structure such as illustrated by **1**. This

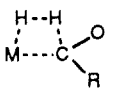

1

reaction mode thus omits the oxidative addition/reductive elimination step. Such a process could also be envisioned for the cobalt system. In fact, Orchin and Rupilius[1b] have on several occations pointed to **1** as a likely transition state in hydrogenolysis involving late transition metals. They have directly implicated[1b] it in step e of the hydroformylation process. Hydrogenolysis in late-transition-metal systems via **1** has also been speculated upon by other workers.[16,17] This reaction mode will be investigated in section V.

The first part of the present study will concentrate on the initial interaction between the coordinatively unsaturated acyl intermediate $CH_3(O)CCo(CO)_3$ and an incoming H_2 molecule. The geometries for the resulting dihydrogen and dihydride complexes will be determined at the Hartree–Fock–Slater level of theory. The second part compares the elimination of aldehyde via oxidative addition, eq 1, and reductive elimination, eq 2, with aldehyde elimination via the four-center intermediary structure, **1**. The energy profiles of the two reaction modes will be investigated by a linear transit procedure.

II. Computational Details

The reported calculations were all carried out by utilizing the vectorized version of the HFS-LCAO program system developed by Baerends et al.[18,19] and vectorized by Ravenek.[19b] The numerical integration procedure applied for the calculations was developed by Becke.[20] All molecular structures were optimized on the singlet energy surface within the C_s symmetry group. The geometry optimization procedure was based on the method developed by Versluis and Ziegler.[21] The electronic configurations of the molecular systems were described by an uncontracted triple-ζ STO basis set[22] on cobalt for 3s, 3p, 3d, 4s, and 4p as well as a double-ζ STO basis set[22] on the ligand atoms. The ligand basis was extended with one polarization function (2p on H and 3d on C and H). The 1s, 2s, and 2p electrons on Co and the 1s electrons on C and O were assigned to the core and treated by the frozen-core approximation.[18] A set of auxilliary[23] s, p, d, f, and g STO functions, centered on all nuclei, was used in order to fit the molecular density and present Coulomb and exchange potentials accurately in each SCF cycle. All calculations were spin-restricted.

Energy differences were calculated by including the local correlation potential by Stoll et al.[24a] and Becke's[24b] nonlocal-exchange corrections. Calculations on metal carbonyls,[25] binuclear metal complexes,[26] and alkyl and hydride complexes,[27] as well as complexes containing M–L bonds for a number of different ligands,[28] have shown that the approximate Density Functional method employed here afford metal–ligand and metal–metal bond energies of nearly chemical accuracy (± 5 kcal/mol). More than 50 molecular structures optimized by Approximate Density Functional theory have been compared with experiment.[21] The

(5) Collman, J. P.; Hegedus, L. S. In *Principles and Applications of Organotransition Metal Chemistry*; Kelly, A., Ed.; University Science Books: Mill Valley, CA, 1980.
(6) (a) Collman, J. P.; Roper, W. R. *Adv. Organomet. Chem.* **1968**, *7*, 53. (b) James, B. R. *Homogeneous Hydrogenation*; Wiley: New York, 1973. (c) Chock, P. B.; Halpern, J. *J. Am. Chem. Soc.* **1966**, *88*, 3511. (d) Halpern, J. *Acc. Chem. Res.* **1970**, *3*, 386.
(7) (a) Lappert, M. F.; Lednor, P. W. *Adv. Organomet. Chem.* **1976**, *14*, 345. (b) Crabtree, R. H.; Morehouse, S. M. *Ibid.* **1982**, *21*, 4210. (c) Harrod, J. F.; Yorke, W. J. *J. Inorg. Chem.* **1981**, *20*, 1156.
(8) (a) Norton, J. *Acc. Chem. Res.* **1979**, *12*, 139. (b) Kemmitt, R. D. W.; Smith, M. A. R. *Inorg. React. Mech.* **1976**, *4*, 3119. (c) Abis, L.; Sen, A.; Halpern, J. *J. Am. Chem. Soc.* **1978**, *100*, 2915. (d) Halpern, J. *Acc. Chem. Res.* **1982**, *15*, 332.
(9) (a) Low, J. J.; Goddard, W. A., III. *Organometallics* **1986**, *5*, 609. (b) Low, J. J.; Goddard, W. A., III. *J. Am. Chem. Soc.* **1984**, *106*, 6228.
(10) (a) Noell, J. O.; Hay, P. J. *J. Am. Chem. Soc.* **1982**, *104*, 4578. (b) Obara, S.; Kitaura, K.; Morokuma, K. *J. Am. Chem. Soc.* **1984**, *106*, 7482. (c) Dedieu, A.; Strich, A. *Inorg. Chem.* **1979**, *18*, 2940. (d) Sevin, A. *Nouv. J. Chim.* **1981**, *5*, 233. (e) Balazs, A. C.; Johnson, K. H.; Whitesides, G. M. *Inorg. Chem.* **1982**, *21*, 2162.
(11) (a) Lauher, J. W.; Hoffmann, R. *J. Am. Chem. Soc.* **1976**, *98*, 1729. (b) Tatsumi, K.; Hoffmann, R.; Yamamoto, A.; Stille, J. K. *Bull. Chem. Soc. Jpn.* **1981**, *54*, 1857. (c) Rabaâ, H.; Saillard, J.-Y.; Hoffmann, R. *J. Am. Chem. Soc.* **1986**, *108*, 4327.
(12) Alemdarogly, N. H.; Penninger, J. L. M.; Oltay, E. *Monatsh. Chem.* **1976**, *107*, 1153.
(13) (a) Kovás, I.; Ungváry, F.; Markó, L. *Organometallics* **1986**, *5*, 209. (b) Ungváry, F.; Markó, L. *Organometallics* **1983**, *2*, 1608. (c) Hoff, C. D.; Ungváry, F.; King, R. B.; Markó, L. *J. Am. Chem. Soc.* **1985**, *107*, 666.
(14) Orchin, M. *Acc. Chem. Res.* **1981**, *14*, 259.
(15) (a) Lin, Z.; Marks, J. *J. Am. Chem. Soc.* **1987**, *109*, 7979. (b) Steigerwald, M. L.; Goddard, W. A.; III *J. Am. Chem. Soc.* **1984**, *106*, 308. (c) Jeske, G.; Lauke, H.; Mauermann, H.; Schumann, H.; Marks, T. J. *J. Am. Chem. Soc.* **1985**, *107*, 8111. (d) Watson, P. J.; Parshall, G. W. *Acc. Chem. Res.* **1985**, *18*, 51.
(16) Joshi, M. A.; James, B. R. *Organometallics* **1990**, *9*, 199.
(17) Brintzinger, H. H. *J. Organomet. Chem.* **1979**, *171*, 337.
(18) Baerends, E. J.; Ellis, D. E.; Ros, P. *Chem. Phys.* **1973**, *2*, 41.
(19) (a) Baerends, E. J. Ph.D. Thesis, Vrije Universiteit, Amsterdam, 1975. (b) Ravenek, W. In *Algorithms and Applications on Vector and Parallel Computers*; Riele, H. J. J., Dekker, Th. J., van de Vorst, H. A., Eds.; Elsevier: Amsterdam, 1987.
(20) Becke, A. D. *J. Chem. Phys.* **1988**, *88*, 2547.
(21) Versluis, L.; Ziegler, T. *J. Chem. Phys.* **1988**, *88*, 322.
(22) (a) Snijders, G. J.; Baerends, E. J.; Vernooijs, P. *At. Nucl. Data. Tables* **1982**, *26*, 483. (b) Vernooijs, P.; Snijders, G. J.; Baerends, E. J. Slater Type Basis Functions for the whole Periodic System. Internal report 1981; Free University: Amsterdam: The Netherlands.
(23) Krijn, J.; Baerends, E. J. Fit functions in the HFS-method. Internal Report (in Dutch), 1984; Free University: Amsterdam, The Netherlands.
(24) (a) Stoll, H.; Golka, E.; Preuss, H. *Theor. Chim. Acta* **1980**, *55*, 29. (b) Becke, A. D. *J. Chem. Phys.* **1986**, *84*, 4524.
(25) Ziegler, T.; Tschinke, V.; Ursenbach, C. *J. Am. Chem. Soc.* **1987**, *109*, 4825.
(26) Ziegler, T.; Tschinke, V.; Becke, A. *Polyhedron* **1987**, *6*, 685.
(27) (a) Ziegler, T.; Tschinke, V.; Becke, A. *J. Am. Chem. Soc.* **1987**, *109*, 1351. (b) Ziegler, T.; Cheng, W.; Baerends, E. J.; Ravenek, W. *Inorg. Chem.* **1988**, *27*, 3458. (c) Ziegler, T.; Tschinke, V.; Baerends, E. J.; Snijdes, J. G.; Ravenek, W. *J. Phys. Chem.* **1989**, *93*, 3050.
(28) Ziegler, T.; Tschenke, V.; Versluis, L.; Baerends, E. J.; Ravenek, W. *Polyhedron* **1988**, *7*, 1625.

agreement between experiment and theory is in most cases excellent.

III. Molecular and Electronic Structures of $CH_3(O)CCo(CO)_3(\eta^2\text{-}H_2)$

The hydrogenolysis of the acyl intermediate in the catalytic hydroformylation reaction, step e of Scheme I, can, as mentioned previously, proceed along a number of conceivable reaction paths. We shall study the process in which aldehyde is formed from an interaction of the coordinatively unsaturated acyl complex with a hydrogen molecule.

The initial outcome of the reaction between the coordinatively unsaturated acyl complex and a hydrogen molecule is conceivably either an η^2-H_2 adduct or a dihydride complex. The structure and stability of the η^2-H_2 adduct will be the subject of the present section whereas the dihydride complex will be scrutinized in the following section. We shall finally discuss in section V how the product from the interaction between H_2 and the coordinatively unsaturated acyl complex can break up into the desired aldehyde as well as the active catalyst $HCo(CO)_3$.

The coordinatively unsaturated acyl complex will be modeled by $CH_3(O)CCo(CO)_3$, which was investigated in detail in a previous study.[4a] It was found in the previous study that the most stable conformation of $CH_3(O)CCo(CO)_3$, **2a**, has the acyl group in the axial position with a

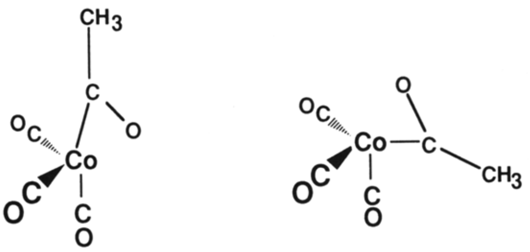

2a **2b**

pronounced η^2 interaction between the acyl oxygen and the metal center. The most stable conformation of $CH_3(O)CCo(CO)_3$ with the acyl group in the equatorial position, **2b**, was calculated to be kJ/mol higher in energy. Complex **2b** exhibits an even stronger η^2 interaction between the acyl oxygen and the metal center than **2a**.

Consideration will be given to the interaction of H_2 with both **2a** and **2b**. In the case of the interaction between **2a** and H_2, two conformations were considered. Structure **2c**

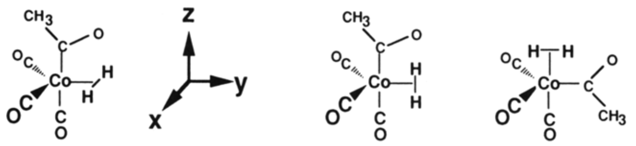

2c **2d** **2e**

has the hydrogens in the equatorial plane; configuration **2d** has them parallel to the apical axis. In the case of the interaction between **2b** and H_2, only one conformation, **2e**, was considered. Structure **2e** has the hydrogens in the axial position and parallel to the Co–C bond of the acyl ligand. We note that H_2 in **2d** and **2e** is ideally positioned for the aldehyde elimination process via the four-center structure **1**, whereas **2c** would have to undergo a rearrangement reaction to **2a**.

The three conformations **2c**–**2e** were found to constitute local minima on the HFS energy surface, and their optimized structures are given in Figure 1. The most stable complex is structure **2c**, which has the hydrogens in the equatorial plane. The reaction **2a** + H_2 → **2c** is nearly thermoneutral with a calculated reaction enthalpy of ΔE = −2 kJ/mol. The reaction is impeded somewhat by the loss of the η^2 interaction in **2a**. The key orbital interaction, **3**, in **2c** is between the metal-based $d_{x^2-y^2}$ HOMO on $CH_3(O)CCo(CO)_3$ and the empty $\sigma^*_{H_2}$ orbital on H_2.

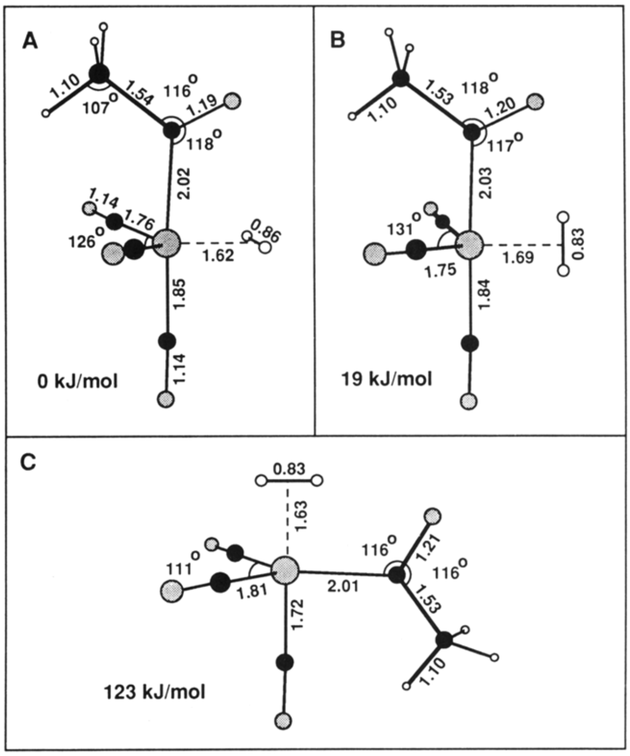

Figure 1. Optimized structures and relative energies of $CH_3C(O)Co(CO)_3(\eta^2\text{-}H_2)$. Bond distances are in Å. The energies are relative to structure A, which was set arbitrarily to zero.

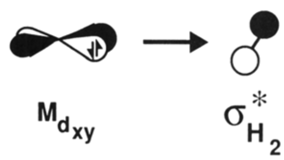

3

Conformation **2d** is only 19 kJ/mol higher in energy with H_2 parallel to the apical axis. The key molecular interaction is now between $\sigma^*_{H_2}$ and the occupied d_{yz} orbital on cobalt. This interaction is somewhat weaker than the corresponding interaction in **3** since the σ nonbonding orbital d_{yz} is of lower energy than the σ antibonding $d_{x^2-y^2}$ orbital.[4b] Conformation **2d** is, as a consequence, less stable than **2c**. However, the energy difference of 19 kJ/mol is sufficiently small to make it feasible for **2c** to convert to **2d**. We calculate the activation barrier for the process **2c** → **2d** to be on the order of 3 kJ/mol.

Structure **2e** is 123 kJ/mol above **2c** in energy and the process **2b** + H_2 → **2e** is calculated to be endothermic with a reaction enthalpy of ΔE = 137 kJ/mol. The unfavorable reaction enthalpy for the process can in part be attributed to a loss of the strong η^2 interaction in **2b**. Further, the key interaction in **2e** between d_{yz} and $\sigma^*_{H_2}$ is weaker than the interaction in **3** since d_{yz} is of lower energy[4b] than $d_{x^2-y^2}$. Our calculations would indicate that the η^2-H_2 adduct **2e** with H_2 in the axial position is much less likely to be formed than the corresponding η^2-H_2 adducts **2c** and **2d** with H_2 in the equatorial position.

The H–H bond distance of the η^2-H_2 adducts is somewhat elongated with respect to the free H_2 molecule where $R(\text{H–H})_{expt}$ = 0.74 Å. The longest bond is found in configuration **2c** with R(H–H) = 0.86 Å, see Figure 1A, while the corresponding H–H bonds in **2d** and **2e** are slightly

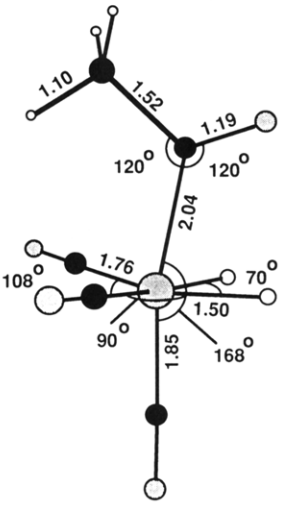

25 kJ/mol

Figure 2. Optimized structure and relative energy of $CH_3C(O)(H)_2Co(CO)_3$. Bond distances are in Å. The energy is relative to $CH_3C(O)Co(CO)_3(\eta^2\text{-}H_2)$, structure A of Figure 1.

shorter with R(H–H) = 0.83 Å, see Figure 1, B and C, respectively. The elongation can be attributed to the electron donation from the metal center into the antibonding σ^* orbital of the hydrogen molecule. The longer R(H–H) bond distance in **2c** is seen to correlate with a corresponding stronger electron donation, **3**, to $\sigma^*_{H_2}$.

Another interesting observation is the increased bond length between the metal center and the acyl ligand in comparison to the coordinatively unsaturated acyl intermediates. Thus, the Co–C_{acyl} bond distances of the optimized structures in Figure 1 are on the average 0.25 Å longer than for the corresponding bonds in the unsaturated compounds.[4a] The increased bond distance can be associated with a weaker bond. This point will obviously be of importance for the aldehyde formation step where the Co–C_{acyl} bond is broken. It should be pointed out that Orchin and Rupilius[1b] postulated the existence of η^2-H_2 complexes as intermediates long before their isolation.[29a] Orchin and Rupilius[1b] were also the first to propose the now widely accepted bonding scheme.

IV. Molecular and Electronic Structures of $CH_3(O)CCo(CO)_3(H)_2$

Next, we shall discuss the product that results from the oxidative addition of H_2 to the unsaturated cobalt complex by way of the most stable η^2-H_2 adduct of configuration **2c**. The structure of the dihydride is represented by **4**, and the optimized geometry is given in Figure 2.

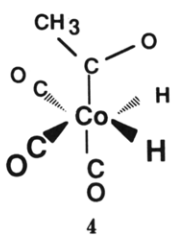

4

We calculate for the dihydride a R(H–Co) bond length of 1.50 Å. This value is 0.17 Å shorter than the corresponding distance in the η^2 complex **2c** but matches the H–Co bond lengths of the monohydride cobalt complexes treated in previous studies.[4] The H–H internuclear distance has increased from 0.86 Å in **2c** to 1.71 Å in **4**. Parallel to the opening of the H–Co–H angle is a reduction

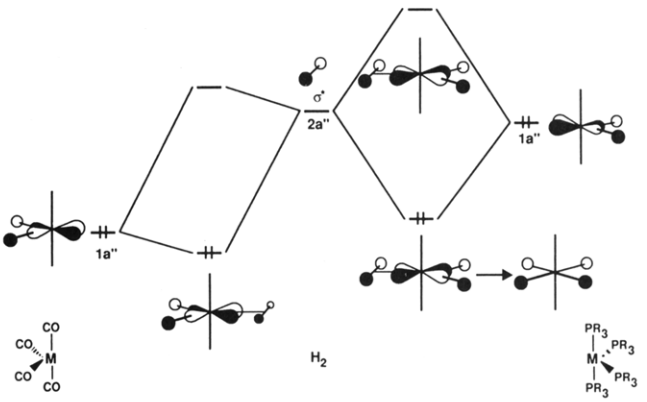

Figure 3. Schematic representation of the HOMO–LUMO interaction between the d^8 complex ML_4 and H_2 for L = CO and L = PR_3. The orbitals are labeled according to C_s symmetry.

of the bond angle between the equatorial carbonyl ligands (126 → 108°); thus, the six-coordinated structure approaches an octahedral geometry. We also notice that the axial groups are somewhat bent toward the hydride ligands. This effect is probably similar to the bending observed for the coordinatively saturated complex $RCo(CO)_4$ (R = H, CH_3), which we have shown in an early study[4a] to be steric in nature.

The dihydride complex of configuration **4** was found to be 25 kJ/mol higher in energy than the η^2 adduct **2c**. Thus, the H_2 complex is more stable than the product of the oxidative addition. In addition, complex **4** is also 6 kJ/mol higher in energy than the η^2 compound **2d**. This result is somewhat surprising since a number of d^8 complexes containing phosphine ligands are known to add H_2 readily, resulting in the formation of dihydrides.[9-11] However, recently thermodynamically stable η^2-H_2 complexes have been prepared.[29,30] The first of these was the d^6 compound $W(P(i\text{-}Pr)_3)_2(CO)_3(H_2)$[29a] for which the H–H distance was found to be 0.75 ± 0.16 Å. A theoretical study[31] on the related model systems $W(PH_3)_2(CO)_3(H_2)$ and $W(PH_3)_5(H_2)$ revealed that the η^2-H_2 complex is stabilized by the π-acceptor CO ligands, which lower the energy levels of the metal d orbitals with respect to the corresponding orbitals in $W(PH_3)_5(H_2)$. As a consequence, the capability of the metal fragment to donate electrons into the antibonding σ^* orbital of the H_2 molecule has diminished, which, in turn, prevents the system from undergoing oxidative addition. It has also been found in experimental studies involving d^8 and d^{10} complexes that the oxidative addition of H_2 is facilitated by electron-releasing ligands such as phosphines and is retarded by π acceptors such as carbon monoxide.[5] In fact, Sweany et al.[32] have quite recently provided evidence for the existence of the d^{10} η^2-H_2 complex $Ni(CO)_3(H_2)$.

We can understand the different role played by the CO and PR_3 ligands in more detail by considering a d^8 complex, ML_4, with a butterfly structure. For this type of

(29) (a) Kubas, G. J.; Ryan, R. R.; Swanson, B. I.; Vergamini, P. J.; Wasserman, H. *J. Am. Chem. Soc.* **1984**, *106*, 451. (b) Kubas, G. J.; Unkefer, G. J.; Swanson, B.; Fukishima, E. *J. Am. Chem. Soc.* **1986**, *108*, 7000. (c) Wasserman, H. J.; Kubas, G. J.; Ryan, R. R. *J. Am. Chem. Soc.* **1986**, *108*, 2294.

(30) (a) Upmacis, R. K.; Gadd, G. E.; Poliakoff, M.; Simpson, M. B.; Turner, J. J.; Whyman, R.; Simpson, A. F. *J. Chem. Soc., Chem. Commun.* **1985**, 27. (b) Sweany, R. L. *J. Am. Chem. Soc.* **1985**, *107*, 2374. (c) Church, S. P.; Grevels, F. W.; Hermann, H.; Schaffner, K. *J. Chem. Soc., Chem. Commun.* **1985**, 30. (d) Crabtree, R. H.; Lavin, M. *J. Chem. Soc., Chem. Commun.* **1985**, 794.

(31) Hay, P. J. *J. Am. Chem. Soc.* **1987**, *109*, 705.

(32) Sweany, R. L.; Polito, M. A.; Moroz, A. *Organometallics* **1989**, *8*, 2305.

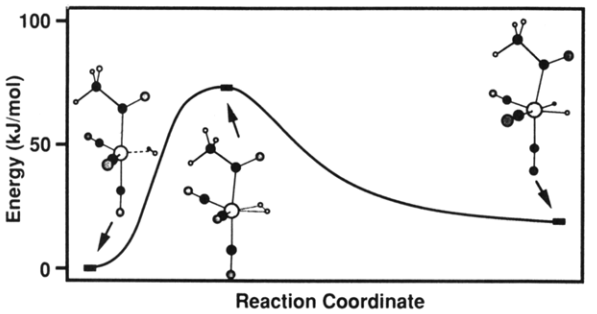

Figure 4. Energy profile of the oxidative addition of H_2 to $CH_3C(O)Co(CO)_3$. Reaction **2c** → **4**. The energy zero point refers to structure **2c**.

metal fragment, the HOMO is a σ antibonding orbital that is mainly d in character; see 1a″ of Figure 3. The HOMO is stabilized strongly in $M(CO)_4$ by π^*_{CO} interactions and to a much lesser extent by $\pi^*_{PH_3}$ interactions in $M(PH_3)_4$, as shown in Figure 3. The energy gap between the HOMO and the vacant σ^* orbital of H_2 is thus larger for a complex containing CO ligands than for the corresponding compound with phosphine groups. Also given in Figure 3 are the interactions between H_2 and ML_4 for L = CO and L = PH_3. In the carbonyl case, the interaction between σ^* and the HOMO of $M(CO)_4$ is small due to the large energy gap. The metal orbital retains as a consequence its d character to a large extent. The situation is quite different for the phosphine complex, where the energy gap between the HOMO and the σ^* orbital is small. The two orbitals can interact well, which results in a substantial lowering of the occupied energy level. The resulting molecular orbital possesses now a M–H bonding and an M–P antibonding ligand–metal combination, which can be correlated to a (essentially) nonbonding ligand–orbital as shown in Figure 3. This means that the d electrons to a large degree have been transferred from the metal center to the equatorial ligands. In other words, the metal complex has been oxidized from a d^8 to a d^6 system. The population of the H_2 σ^* orbital also leads to the cleavage of the H–H bond and the concerted formation of the M–H bonds. This is contrasted by the carbonyl complex where the electrons remain to a large extent in the d-type orbital; thus, the complex does not undergo oxidative addition but forms a stable η^2-H_2 complex.

We have also traced the energy profile for the oxidative addition reaction **2c** → **4**. The profile was obtained by an approximate linear transit procedure in which the internal coordinates of the η^2-H_2 adduct **2c** was changed linearly into the internal coordinates of the dihydride, **4**. A total of eight steps was used in the transit.

The reaction profile for the oxidative addition of H_2 is represented in Figure 4. We find an activation energy ΔE^* of 77 kJ/mol for the reaction **2c** → **4**. This value is markedly larger than the corresponding activation energies determined theoretically for the oxidative addition of H_2 to transition-metal complexes containing phosphine ligands. This can[7] be attributed, as discussed above, to the stabilization of the η^2-H_2 adduct by the π acceptor CO ligands. The energy curve modeled in Figure 4 ascends steeply during the early stages of the reaction, indicating that the activation energy arises largely from the initial elongation of the H–H bond distance.

V. Aldehyde Formation Step by the Four-Center Transition State

As mentioned in the Introduction, there are several conceivable reaction paths along which the aldehyde product can be formed. In this section, we shall concentrate on a mechanism in which one of the hydrogen atoms of the η^2-H_2 complex, **2d**, shifts directly toward the acyl group, thereby forming an aldehyde molecule and regenerating the catalyst $HCo(CO)_3$. The rationale for the study of this particular reaction mode comes from the results of the previous section, where we found the η^2-H_2 adducts **2c** and **2d** to be more stable than the corresponding dihydride, **4**. In addition, this type of reaction mechanism has, to our knowledge, never been investigated theoretically for the cobalt-based hydroformylation process or other electron-rich late-transition-metal centers. On the other hand, this reaction mode is well established among electron-poor early-transition-metal centers in connection with the hydrogenolysis of M–C bonds. The alternative reaction mode via oxidative addition, eq 1, and reductive elimination, eq 2, will be evaluated in the next section.

We will study here the following process. The H_2 molecule of the η^2-H_2 complex with configuration **2d** is moved toward the acyl carbon atom, thereby forming a four-center structure (**2d** → **5a**). Subsequently, the products, $CH_3C(O)H$ and $HCo(CO)_3$, are formed by the cleavage of the H–H and Co–C_{acyl} bonds and the concerted formation of the H–Co and H–C_{acyl} bonds (**5a** → **5b**).

We are not able to investigate the entire reaction surface for the process **2d** → **5a** → **5b**. We shall instead trace an approximate energy profile based on a linear transit pro-

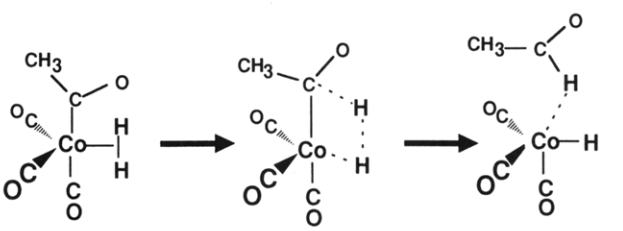

cedure in which optimized structures of **2d**, **5a**, and **5b** are used as fix points. The geometry of **2d** has already been determined; see Figure 1B.

A geometry optimization, starting from the schematic structure in **5a**, revealed an intermediate, **6**, with a distorted four-center geometry. The intermediate represents

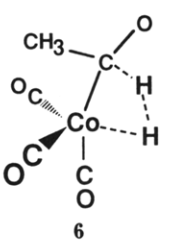

an energy minimum on the energy potential surface with a positive Hessian matrix. The distorted structure, **6**, has the acyl group and the H_2 molecule slightly rotated toward each other. In addition, the H–H and Co–C_{acyl} bonds were somewhat elongated.

The fully optimized geometry of **6** is given in Figure 5. The H–H bond distance in the optimized molecule has increased to 1.14 from 0.83 Å for the η^2 adduct, **2d**. Simultaneously, the internuclear distance between the acyl carbon atom and the nearest hydrogen atom of the H_2 ligand has decreased to 1.37 Å. This value is only approximately 0.30 Å larger than the corresponding C–H bond length in a free acetaldehyde molecule. The optimized geometry of structure **6** shows clearly that the hydrogen atoms, the cobalt center, and the acyl carbon atom all interact with each other. The bonding mode can be explained in the following way. The empty σ^*-H_2 orbital can interact with the occupied orbital on $CH_3(O)CCo(CO)_3$,

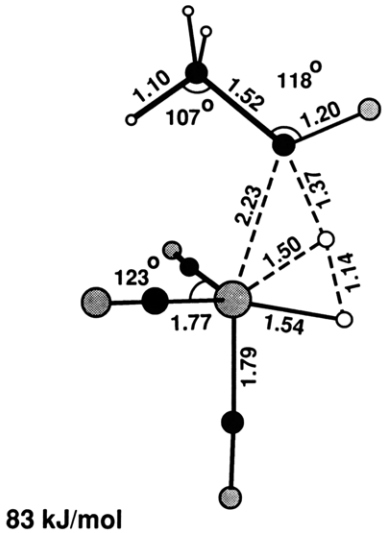

Figure 5. Optimized structure and relative energy of the four-centered intermediate. Bond distances are in Å. The energy is relative to Figure 1B (structure **2d**).

which is responsible for the σ interaction between the acyl group and the metal center. This is illustrated by structure **7a**. Furthermore, the occupied σ orbital of H_2 can still overlap with the LUMO of the butterfly-shaped $CH_3(O)CCo(CO)_3$ fragment, **7b**.

7a **7b**

The distorted complex in Figure 5 was calculated to be 83 kJ/mol higher in energy than the η^2-H_2 complex of configuation **2d**. The lower stability stems (mainly) from the departure of the H_2 group from its preferred orientation in the equatorial site as well as from the bending of the acyl ligand toward the basal position. Structure **6** will be used as the second fix point in tracing the profile for the reaction **2d** → **5a** → **5b**.

We have in order to obtain a third fix point optimized a structure in which the acetaldehyde molecule was somewhat moved away from the metal fragment as indicated by **5b**. The optimization was carried out by keeping the Co–C_{acyl} bond length frozen at 5.0 Å. The optimized geometry is given in Figure 6. We can see clearly that the complex starts to form an acetaldehyde molecule and the coordinatively unsaturated $HCo(CO)_3$ species. The latter approaches **8a**, which is one of the stable configurations

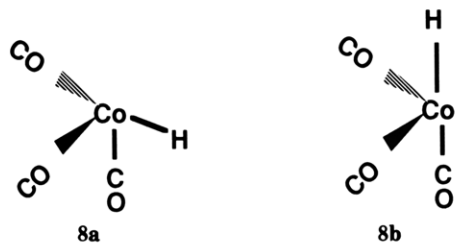

8a **8b**

found in a previous investigation[4a] where we have studied the $HCo(CO)_3$ compound in detail. The acetaldehyde molecule still interacts with the cobalt fragment as revealed by the somewhat elongated H–C_{acyl} bond distance. We find structure **5b**, which has the acetaldehyde molecule almost

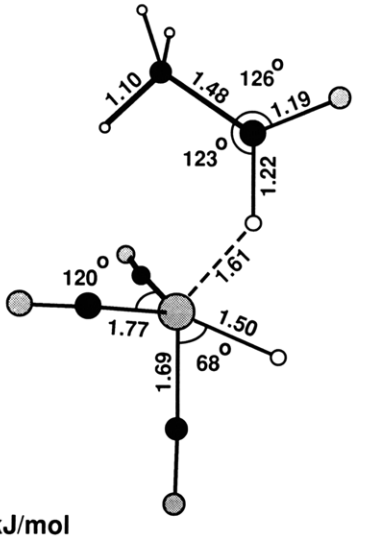

Figure 6. Optimized structure and relative energy of the adduct between acetaldehyde and the cobalt fragment. Bond distances are in Å. The energy is relative to Figure 1B (structure **2d**). The Co–C_{acyl} internuclear distance was kept frozen at 5.0 Å.

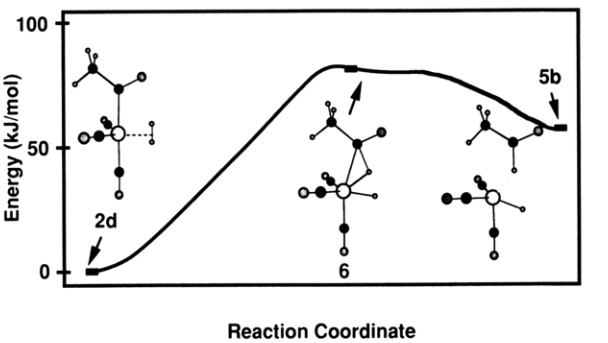

Figure 7. Energy profile for reaction **2d** → **6** → **5b**.

separated from the cobalt catalyst, to be 26 kJ/mol lower in energy than the four-center intermediate **6**.

The approximate profile for the reaction **2d** → **6** → **5b** is given in Figure 7. The first part of the profile connecting **2d** and **6** was obtained by changing the internal coordinates of **2d** into those of **6** in a linear and stepwise fashion. A total of six steps was used in the transit. We find the reaction to proceed with a minimal activation barrier on the HFS energy surface. The activation energy for the first part, **2d** → **6**, is therefore essentially equivalent to the reaction enthalpy ΔE for the reaction **2d** → **6**, which was calculated to be 83 kJ/mol (vide ante). We have also traced the energy surface for the reaction **6** → **5b** by using a similar linear transit procedure with a total of five steps. Step **6** → **5b**, which as already mentioned, is exothermic with a reaction enthalpy of ΔE = −26 kJ/mol and is seen to have a negligible activation energy. This is perhaps not surprising since the H–H and Co–C_{acyl} bonds in structure **6** are already substantially elongated.

Finally, as adduct **5b** breaks up into acetaldehyde and $HCo(CO)_3$ of conformation **8a**, the latter can combine with CO to form $HCo(CO)_4$ of conformation **9a**. The formation

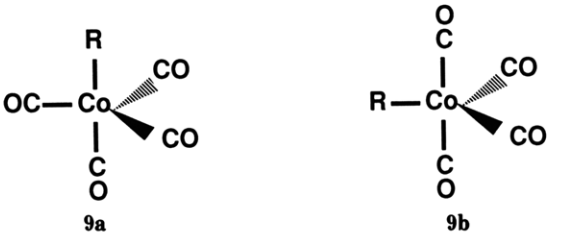

9a **9b**

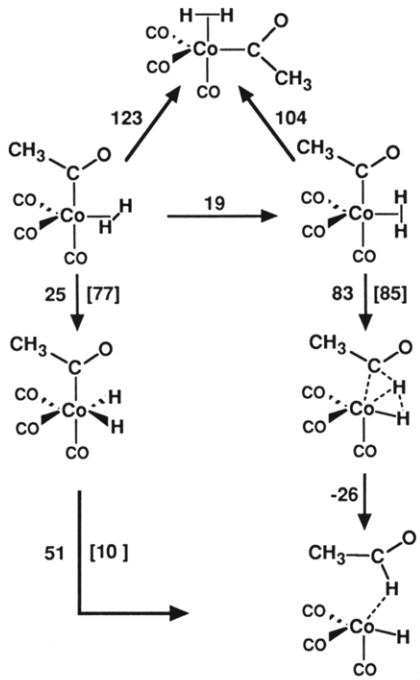

Figure 8. Energy requirements for the rearrangements of $CH_3C(O)Co(CO)_3(\eta^2\text{-}H_2)$. All energies are in kJ/mol. The numbers in brackets represent the activation energies for the reaction in the direction of the arrows. The numbers without brackets stand for the energy difference between two isomers, where a positive value indicates that the resulting complex is higher in energy.

of **9a** is calculated[4a] to be exothermic with $\Delta H = -192$ kJ/mol. The hydride $HCo(CO)_4$ of conformation **9a** can further rearrange to the ground-state conformation, **9b**, with an additional decrease[4a] in energy of 63 kJ/mol. The rearrangement **9a** → **9b** should be facile via a Berry pseudorotation for which the activation barrier typically is less than 25 kJ/mol. The energetics of the various reactions steps have been summarized in Figure 8.

We calculate the overall process in eq 5 to be strongly exothermic with a reaction enthalpy of $\Delta E = -179$ kJ/mol.

$$\mathbf{2c} + H_2 \rightarrow \mathbf{9b} + CH_3(O)CH \qquad (5)$$

The corresponding estimated activation barrier is, as already mentioned, 85 kJ/mol. Note that the starting point in eq 9 is the most stable conformation, **2c**, of $CH_3(O)C\text{-}Co(CO)_3$ and the end point the most stable conformation, **9b**, of $HCo(CO)_4$.

VI. Aldehyde Formation by Reductive Elimination

We have in section V discussed a mechanism for step e of Scheme I involving the four-center transition state, **6**. This mechanism, in which direct oxidative addition of H_2 to the metal center is avoided, has an activation barrier of 85 kJ/mol. We shall now contrast this mechanism for step e with the sequence of oxidative addition, eq 1, and reductive elimination, eq 2, originally suggested by Heck and Breslow.[3]

The profile for the oxidative addition was traced in Figure 4 and found to have an activation barrier of 77 kJ/mol. The energy profile for the reductive elimination process of eq 2, **4** → **5b**, is given in Figure 9. The profile was constructed from a linear transit consisting of six steps. It follows from Figure 9 that the process is endothermic with a reaction enthalpy of 51 kJ/mol. Further, the elimination reaction has a modest activation barrier of less

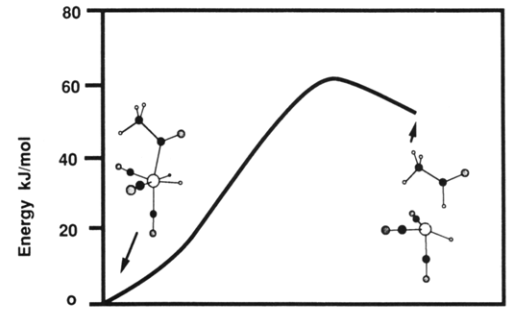

Figure 9. Energy profile for the reductive elimination reaction, **4** → **5b**.

than 10 kJ/mol. It is thus clear that the original mechanism for step e, involving oxidative addition, eq 1, and reductive elimination, eq 2, has an activation barrier of 77 kJ/mol with the oxidative addition being rate determining.

Our calculations would indicate that the two mechanisms proposed for step e have rather similar activation barriers. As a consequence, both mechanisms should be operative. However, the activation barrier for the oxidative addition step of eq 1 will be reduced by substituting CO ligands with phosphines as discussed in section IV. Thus, for the phosphine-substituted cobalt catalysts, $HCo(CO)_2PR_3$, step e might go via a oxidative addition/reductive elemination sequence in which the barrier for the rate-determining oxidative addition step has been diminished. It is interesting to note in closing that step e has been observed[33] to be more facile if one CO ligand is substituted by a phosphine.

VII. Summary and Conclusions

The last step (e) in the catalytic cycle of the hydroformylation process according to Scheme I is the reaction between H_2 and the coordinatively unsaturated acyl intermediate $CH_3(O)CCo(CO)_3$. In this step, acetaldehyde is formed and the catalyst $HCo(CO)_3$ regenerated. Heck and Breslow have suggested that e consists of two processes. The first process, given in eq 1, is an oxidative addition of H_2 to the acyl intermediate $CH_3(O)CCo(CO)_3$, resulting in the dihydride $CH_3(O)CCo(CO)_3(H)_2$. The second process, given in eq 2, represents the reductive elimination of $CH_3(O)CH$ and the regeneration of the catalyst $HCo(CO)_3$. The total activation energy for this sequence was estimated as 77 kJ/mol with the oxidative addition being rate determining.

We found in a study of the oxidative process given in eq 1 that the most stable product from the interaction between the acyl intermediate $CH_3(O)CCo(CO)_3$ and H_2 is the $\eta^2\text{-}H_2$ adduct **2c** rather than the dihydride complex **4**. The finding that the $\eta^2\text{-}H_2$ adduct **2c** is more stable than the dihydride complex **4**, and separated from it by an estimated barrier of 77 kJ/mol, led us to investigate ways in which the $\eta^2\text{-}H_2$ adduct **2c** could decompose into $CH_3(O)CH$ and the catalyst $HCo(CO)_3$ without invoking the prior formation of the dihydride **4**.

The proposed mechanism, which involves a four-center intermediate **6**, has precedence in the hydrogenolysis of M–C bonds containing electron-poor early-transition-metal centers. It has not been considered extensively in connection with electron-rich late transition metals. We have found that the conversion of the $\eta^2\text{-}H_2$ adduct **2c** into $CH_3(O)CH$ and the catalyst $HCo(CO)_3$, via the four-center

(33) (a) Masters, C. *Homogeneous Transition-metal Catalysis*; Chapmann and Hall: New York, 1980. (b) Paulik, F. E. *Catal. Rev.* **1972**, *6*, 49.

intermediate **6**, is fiasable, with an estimated activation barrier of 85 kJ/mol. It is further concluded that both the oxidative addition/reductive elimination sequence and the process involving the four-center intermediate **6** are likely candidates as mechanisms for step e of Scheme I. The mechanism involving the four-center intermediate **6** was first proposed by Orchin and Rupilius[16] in connection with step e of the hydroformylation process.

The calculated activation barriers for step e of 75–85 kJ/mol are comparable to the barrier of 80 kJ/mol calculated[4a] for the migratory insertion step d of Scheme I. They are further smaller than the 186 kJ/mol[4a] required in step a. The latter finding can be reconciled with the experimental observation that the hydrogenolysis of R-(O)CCo$(CO)_3$P(n-Bu)$_3$ is substantially retarded[34] in the presence of carbon monoxide.

Acknowledgment. This investigation was supported by the Natural Sciences and Engineering Research Council of Canada (NSERC). We also acknowledge access to the Cyber-205 installations at the University of Calgary. We are thankful to Professor E. J. Baerends and Professor W. Ravenek from the Free University of Amsterdam for a copy of their latest vectorized version of the HFS-LCAO program system. We would also like to thank Pieter Vernooijs for help with the installation of the program system.

(34) Piacenti, F.; Bianchi, M.; Benedetti, E. *Chim. Ind. (Milan)* **1967**, *14*, 205.